Mechanical and elastic properties of new silicon nitride ceramics produced by cold isostatic pressing and free sintering

O. Lukianova*

Belgorod National Research University, Center of the Structural Ceramics and Engineering Prototyping, 85, Pobedy Street, 308015 Belgorod, Russia

Abstract

The mechanical and elastic properties of new silicon nitride fabricated by cold isostatic pressing and free sintering are considered. Young's modulus, Poisson's ratio and shear modulus of investigated ceramic were determined. An indentation technique for measuring the indentation modulus was developed. The flexural strength, the compressive strength and the fracture toughness were investigated. Young's modulus of the obtained material was 240 GPa by resonance and 214 GPa by mechanical tests. The microhardness was 1380 $HV_{0.5}$ and 970 $HK_{2.5}$. Obtained silicon nitride ceramic is one of a candidate material for a wide range of structural applications due to its high density (2.94 g/cm^3) and low open porosity (0.1%).

1. Introduction

Silicon nitride ceramics are frequently used as structural and engine components for high-temperature applications. They exhibit unique properties including high levels of the high fracture toughness, strength, thermostability, hardness and chemical stability at room and high temperatures [1]. Much of the research and development has been focused on the fabrication of ceramic bodies [2]. The silicon nitride ceramics are produced by different methods, such as sintering, reaction bonding (RB), hot pressing (HP), hot isostatic pressing (HIP) and spark plasma sintering (SPS) [3]. The high-temperature mechanical properties such as bending strength, tensile strength, fracture toughness, and thermal properties have been extensively studied. [1]. Nowadays, there are two main tasks in the ceramic industry – the improvement in reliability and the reduction of production costs [4]. The cold isostatic pressing is one of the most realistic approaches for tackling these tasks [5]. The most ceramic components are assembled with the

metallic ones to use the advantageous properties of each material. It should be noted that the thermal expansion coefficients for ceramic and metal are different, which may results in fracture of the ceramic components by the thermal stresses. It is highly desirable, therefore, to reduce Young's modulus of the ceramics without sacrificing the strength to overcome this problem [6].

The investigated material can be used as an economically and functionally superior alternative to other types of commercial silicon nitride in a wider range of potential commercial applications. The aim of the current study is to clarify the elastic and mechanical properties including Young's modulus, flexural strength and fracture toughness of the investigated material. These properties remain unclear and have attracted much interest.

2. Experimental

2.1. Materials and methods

The starting materials were powders of 85 wt% silicon nitride (Stark, Grade M11), 6 wt% Y_2O_3 (Grade B), and

---

*Tel./fax: +7 4722 261477.

E-mail address: sokos100@mail.ru

9 wt% Al_2O_3 (A 16 SG Grade, Alcoa). The powder mixture was ground in an atrittor mill (Retsch RS-200) for 24 h. The ground and homogenized powder mixture was cold isostatically pressed at 200 MPa (EPSI CIP 400 B-9140 press). Conventional sintering of the samples was carried out in a high temperature furnace (Nabertherm VHT 8/22-GR) in nitrogen atmosphere at 1650 °C for 60 min. More experimental details are described in Ref. [7] and RU Patent no 2014127439.

2.2. Test specimens

The specimens were cut, mechanically machined and polished using 3-micron diamond suspension. Compression and bending tests were carried out using an Instron 300 LX testing machine at room and elevated temperatures in air up to 500 °C. Bar specimens ($6.4 \times 7.2 \times 50$ mm^3 and $5.6 \times 9.6 \times 9.9$ mm^3) were used for bending and compression tests. The samples were broken in 3-point-bending (3PB) mode with the loading distance 30 mm. Maximum strength, σ_b and σ_c were determined using the maximal applied load. At least eight specimens were tested under the same conditions. In all the experiments, the speed of the testing machine crosshead was constant and equal to 0.5 mm/min.

For both the Vickers and Knoop indentations, the samples of approximately 60 mm × 20 mm × 30 mm in size were polished with diamond paste on a standard metallographic wheel, using 6 and 3 μm diamond pastes to achieve a mirror-like surface finish that contained quite small number of well-dispersed very fine pores. Both Knoop and Vickers indentations were made at 5 and 25 N loads using an Indenter test – Device (construction and software self-made microindentation hardness tester) and a loading time of 15 s. The indentation sizes and the Vickers indentation crack lengths were measured immediately after unloading using an optical microscope Keyence VHX-500. Only perfect indentations, those with clearly symmetrical indentations and with symmetrical crack patterns, were utilized in the final calculations, a point which will be addressed later in this paper. A total of 25 perfect indentations were made at each load with the Vickers indenter. Also 25 Knoop indentations were taken for a separate hardness characterization, for hardness enters into all of the proposed equations. The characteristic lengths, were measured along both diagonal directions of the Vickers pyramids, yielding 50 values at each test load. The indentation modulus was calculated from the load–displacement curve.

Critical stress intensity factor, or fracture toughness, K_{IC}, was measured by the indentation fracture (IF) method. The specimens were indented on the polished surface with a Vickers microhardness tester using loads from 350 to 400 N.

Density of the samples was determined by the helium pycnometer (Micromeritics AccuPyc 1340) and by the Archimedes method. Bulk density, apparent density, open porosity and pore size distribution were determined by the mercury intrusion porosimetry.

Young's modulus, shear modulus and Poisson's ratio were measured by the resonance method according to ASTM C 1259-01 using Gindosonic, Type Mk5I. Disc-shaped samples with a diameter of 44 mm and a thickness of 3 mm were used. Also Young's modulus was measured by 4PB tests with strain gauges. Bar samples ($2.7 \times 4.1 \times 40$ mm^3) were used. Mechanical tests were carried out with an inner span of 20 mm, an outer span of 35 mm and a crosshead speed of 0.5 mm/min at room temperature.

The indentation modulus was calculated by the Oliver and Pharr method [8]. One of the most important factors that determines the correct calculation of the indentation modulus is compliance of the machine. Ulner and others [9] described the method of calculation of the machine compliance and correct zero point. It was based on the analysis of measured depth from the load $F^{0.5}$ dependence. It was necessary to calculate the polynomial of the second order. The first coefficient of this polynomial gave the machine compliance and the last coefficient gave real zero point, respectively.

The indentation depth, h, was calculated according to Ref. [10] by the equation:

$$h = h_{meas} - h_0 - C_m \cdot F_{max} \tag{1}$$

where h_{meas} is the indentation depth, μm, C_m is the compliance of the machine, μm/N, F_{max} is maximum load, N, h_0 is correct zero point, μm. The maximum depth of the indentation h_{max} and stiffness were calculated from the load–displacement curve.

The plastic indentation depth, h_c, was calculated according to [10]

$$h_c = h_{max} - \frac{\varepsilon \cdot F_{max}}{S} \tag{2}$$

where S – stiffness, $\varepsilon = 0.75$ for Vickers indenter.

The indentation modulus E_{IT} was calculated by

$$E_{IT} = \frac{S \cdot \sqrt{\pi}}{2 \cdot h_c \cdot \sqrt{G}} \tag{3}$$

where G for Vickers indentor is about 26.43 [9].

3. Results and Discussion

3.1. Physical properties

All specimens were sintered to near full density (Table 1). The linear shrinkage of the sintered silicon nitride was 13%. The mercury intrusion porosimetry results are shown in Table 1. It can be noticed that obtained ceramic had high bulk and apparent density of 2.938 g/cm^3 and 2.941 g/cm^3, respectively, and low open porosity (0.115%). It should however be noted, that the average size of the open pores was 9.2 μm (Table 1). The density amounted to 2.94 g/cm^3 by helium pycnometry and Archimedes method. For comparison, the

Table 1
Physical properties.

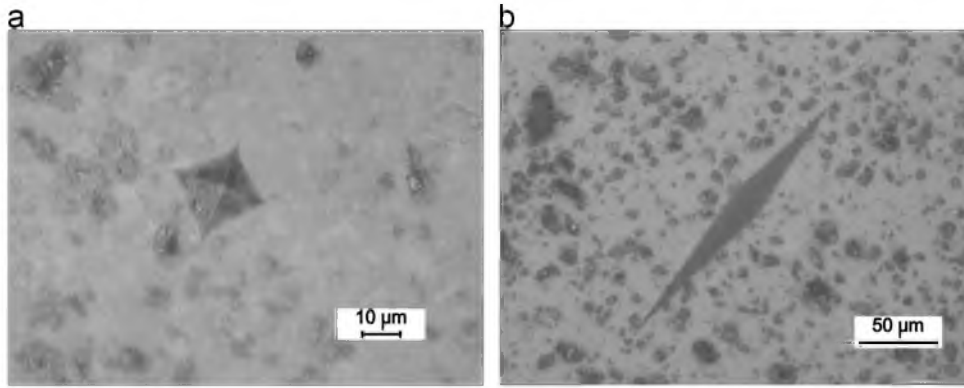| Bulk density (g/cm^3)	Open porosity (%)	Apparent density (g/cm^3)	Average pore diameter (μm)
2.938	0.115	2.941	9.213

Fig. 1. Vickers (a) and Knoop (b) indentations.

Table 2
Mechanical characteristics.

Microhardness (± 15 HV$_{0.5}$)	Microhardness (± 15 HK$_{2.5}$)	Bending strength (σ_b, MPa)	Compressive strength (σ_c, MPa)	K_{1C} (MPa/m$^{-1/2}$)
1380	970	280	2200	6

open porosity of the silicon nitride based ceramics, obtained by RBSN varied from 6.6% to 21.5%. The density of this material ranged from 2.25 to 2.65 g/cm^3 and the size of the open pores varied from 0.03 to 0.15 μm [11,12]. It is obvious, that the density of ceramics depends on porosity and on the pore size. Thus, the ceramics produced by SPS and HIP methods has the highest density close to the theoretical one [13,14].

3.2. Mechanical properties

Fig. 1a and b illustrates two typical print patterns, which were observed for the Vickers and Knoop indentations in this study. An indentation load has been chosen experimentally for the both methods. The microhardness of the obtained material was 1380 HV$_{0.5}$ by Vickers and 970 HK$_{2.5}$ by Knoop (Table 2). Silicon nitride ceramics a priori have high hardness [15]. It is well known, that microhardness of ceramics depends on producing method [16]. Therefore, ceramics produced by HIP, HP, GPS and SPS have higher microhardness than the same ceramics produced by RBSN and pressureless sintering methods. For example, the microhardness of the materials obtained by HP was 1733 HV [17], while the microhardness of the RBSN ceramics was 1020 HV [3]. The microhardness of ceramics obtained by SN varied from 850 HV to 1330 HV.

In spite of some disadvantages [18], IF method is one of the most popular methods to determine the fracture toughness of brittle materials due to its convenient and nondestructive character [19]. The Vickers indentations with well-developed Palmqvist cracks are observed in Fig. 2. There were no cracks from 1 to 10 N for Knoop indentations. This fact is most likely associated with a penetration depth of the Vickers indenter. It is well known that Vickers indenter is much deeper than Knoop indenter at the similar test loads. For example, the unrecovered depth of the Vickers indentation at 3 N is nearly equal to that of
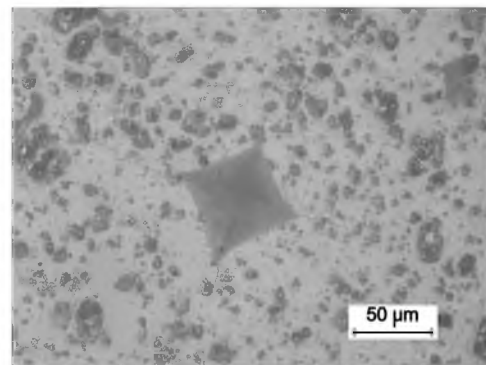
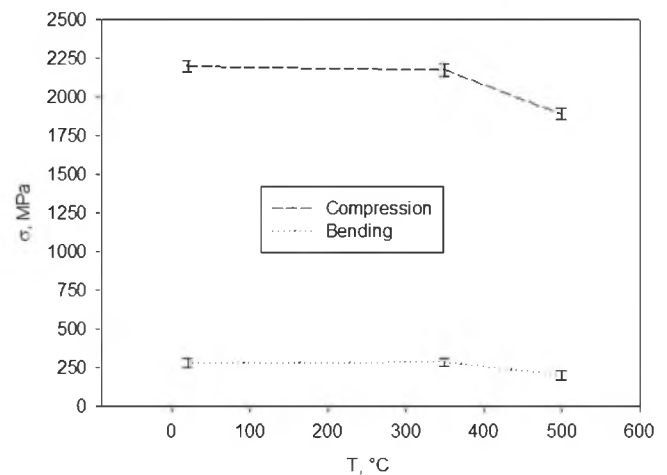

Fig. 2. Vickers indentation with Palmqvist cracks.

Fig. 3. High-temperature test results.

a Knoop indentation at a 10 N load. The fracture toughness of the investigated ceramic was calculated for Palmqvist cracks by Niiahara equation [20]. The fracture toughness of the obtained ceramic was 6 MPa/m$^{-1/2}$ according to this equation.

The high temperature dependences of the bending and compression strength from 20 °C to 500 °C are shown in Fig. 3. Primarily, it is shown that the shapes of the curves were typical and the same in the both cases. It should be noted that the highest strength was observed at the lowest temperature for the both tests. In particular, the maximum bending strength, σ_b 280 MPa and the maximum compressive strength σ_c, 2200 MPa
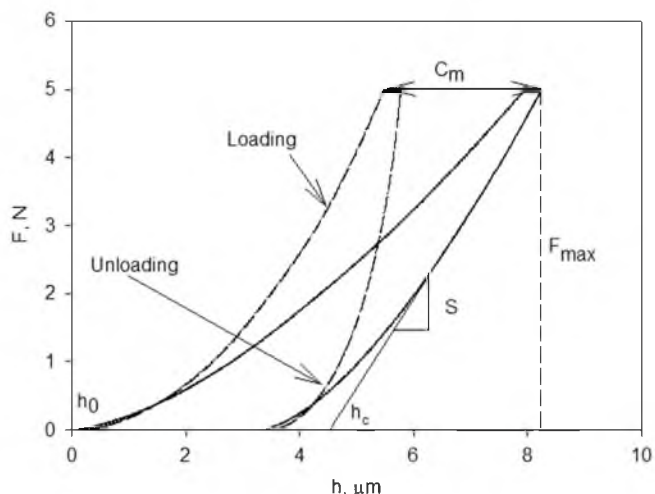
Fig. 4. Load–displacement curve.

Table 3
Elastic properties.

Method	Resonance	4PB
E (GPa)	240	214
G (GPa)	90	84
ν	0.28	0.28

were observed at room temperature (Fig. 3). The strength decreases insignificantly with an increase in the temperature from 20 °C to 350 °C. Further increase in the testing temperature up to 500 °C is accompanied with a decrease in the strength of ceramic ($\sigma_c = 1865$ MPa and $\sigma_b = 204$ MPa, Fig. 3). For comparison, the bending strength of Si_3N_4 based ceramics obtained by HIP was 800 MPa and decreased down to 351 MPa with 10 wt% graphene additive. Also, it has to be mentioned that graphene led to decreasing the microhardness of this ceramic from 1305 HV to 744 HV. The fracture toughness varied from 8.2 MPa/m$^{-1/2}$ to 4.9 MPa/m$^{-1/2}$ [21]. The bending strength of the RBSN ceramics was 82–182 MPa and its fracture toughness was 1.36–2.78 MPa/m$^{-1/2}$ [22]. The bending strength of the samples obtained by RBSN varied from 150 to 250 MPa at room temperature [21].

3.3. Elastic properties

Silicon nitride ceramics have a high Young's modulus [3]. Elastic constants of the silicon nitride ceramics depend on the porosity and, consequently, on the density. The elastic modulus data are given for silicon nitride ceramic with density 2.94 g/cm^3. Usually, as the porosity dependence of Young's modulus can be expressed by an exponential relationship, the modulus can decrease by half with 0.2–0.3 porosity.

As it was noted above, the elastic properties (Young's modulus, shear modulus, Poisson's ratio) of ceramics, as well as the mechanical properties, depend on the method of ceramic processing. For example, Young's modulus of the RBSN ceramics varied from 160 GPa to 200 GPa ($\nu = 0.23$), while

Young's modulus of the HIP ceramics was twice higher ($E = 320$ GPa, $\nu = 0.28$) [3].

Thus, the indentation modulus of the investigated material was 244 GPa. Load–displacement curve is shown in Fig. 4. Usually, the indentation modulus has the same value as Young's modulus. For comparison, Young's modulus of the investigated material was 240 GPa by resonance tests (Table 3).

Young's modulus was 190 GPa according to Marshall, Blau and Lima equation [23]. At the same time, Young's modulus by 4PB was 214 GPa, shear modulus was 84 GPa and Poisson's ratio was 0.28 (Table 3). For comparison, Young's modulus of the silicon nitride obtained by uniaxial pressing was 161 GPa [4].

4. Conclusions

In conclusion, the silicon nitride ceramic was produced by the cold isostatic pressing via free sintering. The mechanical and elastic characteristics of the produced ceramic were investigated. It should be noted that the properties of the produced material are higher than properties of the reaction bonded silicon nitride but lower than characteristics of the material obtained by HIP and SPS. Moreover it is obvious that the proposed method is much cheaper than HIP and SPS. Proposed technology can be potentially applied in various fields of technology and industry in production of structural ceramics based on silicon nitride.

The results can be summarized as follows:

1. The density of the obtained material was 2.94 g/cm^3. The open porosity was 0.1%. However, the average pore size of the open pores was about 9.2 μm.
2. The microhardness of the obtained ceramic was 1380 HV$_{0.5}$ and 970 HK$_{2.5}$. The bending strength, σ_b, was 280 MPa and compression strength σ_c was 2200 MPa. The fracture toughness of the material was 6 MPa/m$^{-1/2}$.
3. Young's modulus decreases with an increase in temperature. It was 214 GPa by 4PB and 240 GPa by resonance. Poisson's ratio (0.28) and shear modulus (90 GPa) were determined. The indentation modulus calculated from the loading curve was 244 GPa.

References

[1] M. Shimada, M. Matsushitas, H. Kuratan, T. Kamoto, M. Tsukuma, T. Ukidate, Temperature-dependence of young modulus and internal-friction in alumina, silicon-nitride, and partially stabilized zirconia ceramics, J. Am. Ceram. Soc. 67 (2) (1984) 23–24.

[2] A. Hasnat Hosneara, A.H. Bhuyan, Structural and electrical properties of silicon nitride ceramic, Daffodil Int. Univ. J. Sci. Technol. 7 (1) (2012) 50–58.

[3] D. Munz, T. Fett, Ceramics: Mechanical Properties, Failure Behavior, Materials Selection, Springer series in Materials Science, vol. 36, Springer-Verlag, Berlin, 1999, p. 298.

[4] T. Hotta, H. Abe, T. Fukui, M. Naito, N. Shinohara, K. Uematsu, Effect of dewaxing procedures of cold isostatically pressed silicon nitride ceramics on its microstructure and fracture strength, Adv. Powder Technol. 14 (5) (2003) 505–517.

[5] J. Luo, C. Zhang, H. Ma, G. Wang, Cold isostatic pressing–normal pressure sintering behavior of amorphous nano-sized silicon nitride powders, Adv. Mater. Res. 454 (2012) 17–20.

[6] M. Brito, H.-T. Lin, K. Plucknett, Silicon-Based Structural Ceramics for the New Millennium, 142, , 2003.

[7] V.V. Krasil'nikov, V.V. Sirota, A.S. Ivanov, L.N. Kozlova, O.A. Luk'yanova, V.V. Ivanisenko, Investigation of the structure of Si_3N_4-based ceramic with Al_2O_3 and Y_2O_3 additives, Glass Ceram. 1 (2014) 17–19.

[8] W.C. Oliver, G.M. Pharr, A new improved technique for determining hardness and elastic modulus using load and sensing indentation experiments, J. Mater. Res. 7 (6) (1992) 1564–1582.

[9] C. Ullner, E. Reimann, H. Kohlhoff, A. Subaric-Leitis, Effect and measurement of the machine compliance in the macro range of instrumented indentation test, Measurement 43 (2010) 216–222.

[10] C. Ullner, HARDMEKO 2004 hardness measurements theory and application in laboratories and industries 11–12 November, Washington, D.C., USA, critical points in ISO 14577 part 2 and 3 considering the uncertainty in measurement, 2004.

[11] G. Ziegler, J. Heinrich, G. Wötting, Review relationships between processing, microstructure and properties of dense and reaction-bonded silicon nitride, J. Mater. Sci. 22 (9) (1987) 3041–3086.

[12] ⟨http://www.azom.com/article.aspx?ArticleID=77⟩.

[13] H. Peng, Spark Plasma Sintering of Si_3N_4-Based Ceramics – Sintering Mechanism-tailoring Microstructure-Evaluating Proper Doctoral Dissertation, Department of Inorganic Chemistry Stockholm University, Stockholm Sweden, 2004.

[14] K. Berroth, Silicon nitride ceramics for product and process innovations, Adv. Sci. Technol. 65 (2005) 70–77.

[15] M.H. Bocanegra-Bernal, B. Matovic, Dense and near-net-shape fabrication of Si_3N_4 ceramics, Mater. Sci. Eng. A 500 (2009) 130–149.

[16] C. Guedes-Silva, F. de Souza Carvalho, J. Bressiani, Effect of rare-earth oxides on properties of silicon nitride obtained by normal sintering and sinter-HIP, J. Rare Earths 30 (11) (2012) 1177–1183.

[17] A.K. Mukhopadhyay, S.K. Datta, D. Chakraborty, On the microhardness of silicon nitride and sialon ceramics, J. Eur. Ceram. Soc. 6 (5) (1990) 303–311.

[18] G.D. Quinn, R.C. Bradt, On the Vickers indentation fracture toughness test, J. Am. Ceram. Soc. 90 (3) (2007) 673–680.

[19] A.C. Fischer-Cripps, Introduction to Contact Mechanics (Mechanical Engineering Series), , 2000, p. 243.

[20] K. Niihara, R. Morena, D.P.H. Hasselman, J. Mater. Sci. Lett. 1 (1) (1982) 13–16.

[21] P. Rutkowski, L. Stobierski, D. Zientara, L. Jaworska, P. Klimczyk, M. Urbanik, The influence of the graphene additive on mechanical properties and wear of hot-pressed Si_3N_4 matrix composites, J. Eur. Ceram. Soc. 35 (1) (2015) 87–94.

[22] D. Yao, Y. Xia, K. Zuo, D. Jiang, J. Günster, Y. Zeng, J. Heinrich, The effect of fabrication parameters on the mechanical properties of sintered reaction bonded porous Si_3N_4 ceramics, J. Eur. Ceram. Soc. 34 (15) (2014) 3461–3467.

[23] D.B. Marshall, T. Noma, A.G. Evans, A simple method for determining elastic-modulus-to hardness ratios using Knoop indentation measurements, J. Am. Ceram. Soc 65 (1982) 175.